



ARTICLE

Protein Disulfide Isomerase and Its Potential Function on Endoplasmic Reticulum Quality Control in Diatom *Phaeodactylum tricornerutum*

Yanhuan Lin^{1,#}, Hua Du^{2,#}, Zhitao Ye², Shuqi Wang², Zhen Wang² and Xiaojuan Liu^{2,*}

¹Zhangzhou Institute of Technology, Zhangzhou, China

²Guangdong Provincial Key Laboratory of Marine Biotechnology, Guangdong Provincial Key Laboratory of Marine Disaster Prediction and Prevention, College of Sciences, Shantou University, Shantou, China

*Corresponding Author: Xiaojuan Liu. Email: liuxiaojuan@stu.edu.cn

#These authors contributed equally to this work

Received: 14 August 2023 Accepted: 28 November 2023 Published: 26 January 2024

ABSTRACT

PDI is a molecular chaperone and plays an important role in Endoplasmic Reticulum quality control (ERQC). PDI participates in the refolding of the misfolded/unfolded proteins to maintain cellular homeostasis under different stresses. However, bioinformatic characteristics and potential functions of PDIs in diatom *Phaeodactylum tricornerutum* (Pt) are still unknown so far. Hence, the genome-wide characteristics of PtPDI proteins in *P. tricornerutum* were first studied via bioinformatic and transcriptomic methods. 42 PtPDI genes were identified from the genome of *P. tricornerutum*. The motif, protein structure, classification, number of introns, phylogenetic relationship, and the expression level of 42 PtPDI genes under the tunicamycin stress were analyzed. A pair of tandem duplicated genes (PtPDI15 and PtPDI18) was observed in *P. tricornerutum*. The 42 PtPDIs with different gene characteristics were divided into three independent clades, indicating different evolutionary relationships and functions of these PtPDIs. The 14 up-regulated PtPDI genes under the tunicamycin treatment might have a positive effect on the ER quality control of the unfolded/misfolded proteins, while the 7 down-regulated PtPDIs might negatively affect the ERQC. The characteristics of all 42 PtPDIs and their proposed working model here provide a comprehensive understanding of the PtPDIs gene family. The differential expression of 21 PtPDIs will be useful for further functional study in the ERQC.

KEYWORDS

Protein disulfide isomerase; gene family; Endoplasmic Reticulum quality control; *Phaeodactylum tricornerutum*

1 Introduction

Molecular chaperones are the guardians of protein homeostasis [1]. They widely exist in eubacteria archaeobacteria and eukaryotic cells [2]. Molecular chaperones could interact with another protein to form its functional active conformation [3]. Previous studies have already shown that molecular chaperones are essential for cellular protein folding, refolding, and the ubiquitin-proteasome system, playing an important role in removing the misfolded and aggregated proteins timely under stresses [4]. Additionally, molecular chaperones could promote cell survival in a non-physiological state and stressful conditions by preventing



aggregation and promoting refolding of proteins. It was reported that these functions are ubiquitous and conserved in all organisms [1].

Protein disulfide isomerases (PDIs), a kind of 55 kDa proteins, are important molecular chaperones in the Endoplasmic Reticulum quality control (ERQC). ERQC is known as a calreticulin/calnexin cycle and plays a key role in glycoprotein folding, secretion, and maturity [5,6]. The ERQC recognizes the misfolded/unfolded proteins on the way to their secretory pathway [7]. In the ERQC, together with the ER lectins calnexin (CNX) and/or calreticulin (CRT), molecular chaperones (e.g., PDIs) combine to the N-linked mono-glucosylated glycan of glycoproteins and aid the folding of glycoproteins [5]. The structure of PDIs was widely studied in plants. The PDIs are composed of five domains, including a, b, b', a', and c domains. There are two active sites in the a and a' domains, both have two cysteine residues [8]. The a-type domain carrying the "Cys-Gly-His-Cys" motif contains catalytic active sites and plays a role in the reduction-oxidation cycle. The b-type domain is enriched in hydrophobic residues, involving substrate binding. It was reported that PDIs are a kind of thiol oxidoreductase chaperones located in the ER [9]. It was shown that PDIs are divided into three classes in microalgae. The first class contains a central Trx module with a canonical YAPWCGHC active site sequence. The second class harbors an N-terminal Trx domain with a variable active site sequence. The third class has two domains, a N-terminal Trx domain and a long α -helix domain at the C-terminus [10]. For example, Rb60 in *Chlamydomonas reinhardtii*, the third class of PDI protein, contains two thioredoxin-like domains with a putative catalytic site of "-Cys-Gly-His-Cys-" [11]. Although characteristics of PDIs were compared between plants and chromalveolates [12], however, the structure of PDIs and their characteristics in microalgae, including the conserved motifs and domains, classification, the number of introns-exons, and phylogenetic relationship are still unknown so far.

Additionally, PDIs display different functions in plants. The classical function of PDI proteins is responsible for the introduction or isomerization of disulfide bonds in nascent ER proteins, aiding the refolding of misfolded/unfolded proteins, and finally retaining the protein homeostasis [8,11,13]. For example, AtPDIs located in chloroplasts of leaves are associated with starch granule biosynthesis in *Arabidopsis thaliana* [14]. In Soybean DG330, the upregulated expression of the GmPDIL7 gene helps the formation of disulfide bonds in nascent proteins under ER stress [15]. *SIPDI* (Protein disulfide isomerases of *Solanum Lycopersicum*) promotes the tomato resistance to TYLCV virus by reducing hydrogen peroxide (H_2O_2) levels, increasing the activity of superoxide dismutase (SOD) and peroxidase (POD), and enhancing antioxidant activity. It was indicated that SIPDI plays an essential role in enhancing the protein folding function of ER and promoting the synthesis and conformation of antioxidant-related proteins [16]. In addition to plants, the function of PDIs in microalgae was also studied. In *C. reinhardtii*, Rb60 regulates the translation of proteins and can maintain photosynthesis. CrPDI2 is a redox-active protein in *C. reinhardtii*. It was found that CrPDI2 participates in the regulation of the circadian signaling pathway [17]. So far, a lot of PDI studies have been focused on Chlorophyta, such as *C. reinhardtii*. However, the expression characteristics and function of the PDI gene family in diatom remain unknown.

Phaeodactylum tricornerutum, a diatom, is one of the most important primary producers in the ocean [18]. In this study, *P. tricornerutum* was used to study the conserved motifs, gene structures and the distribution of genes on the chromosomes, evolutionary relationship, and putative function of PtPDIs via bioinformatic analysis and molecular biotechnology. Tunicamycin is an effective inhibitor of protein N-glycosylation to disrupt the N-glycosylation modification of proteins in organisms [19]. N-glycosylation is an important co- and post-translational event in the modification of proteins in eukaryotes. N-glycosylation plays a vital role in the function of protein. In *P. tricornerutum*, the pathway of protein N-glycosylation mainly takes place in the ER and Golgi apparatus [14]. The stress of tunicamycin will disrupt protein homeostasis. Therefore, it is valuable to study the expression characteristics of PDIs and propose their

potential functions under tunicamycin stress. The results obtained in this study will provide an important foundation for clarifying the mechanism of PDIs proteins in protein homeostasis [20].

2 Materials and Methods

2.1 Microalgae and Growth Conditions

P. tricornutum (Pt1, obtained from Oil Crops Research Institute of Chinese Academy of Agricultural Sciences, China) was cultured in f/2 medium and placed in a 16 h light and 8 h dark culture environment with a speed of 100 rpm and a light intensity of 30–40 $\mu\text{mol photons}\cdot\text{m}^{-2}\cdot\text{s}^{-1}$ at $25 \pm 1^\circ\text{C}$.

2.2 Bioinformatic Analysis of PtPDI Gene Family

2.2.1 Mining and Identification of PtPDI Gene Family in *P. tricornutum*

cDNA, PEP (phospholipid exchange proteins), CDS (Coding sequence), and GFF (Generic Feature Format) files were downloaded from the Ensembl database (<http://www.protists.ensembl.org>). The hidden Markov model (HMM) file of the PtPDI gene family (Pfam number: PF0085) was downloaded from the Pfam database (<http://pfam.xfam.org/>). Based on these data, PDI candidates were screened via the domain search (e-value < 3.8e-06) from the *P. tricornutum* genome. The PDI candidates were manually validated on the NCBI, CDD (<https://www.ncbi.nlm.nih.gov/CDD/>), and SMART (<http://www.smart.embl.de>) websites to ensure that each gene has the thioredoxin domain.

2.2.2 Phylogenetic Tree and Conserved Motif Domain, Gene Structure Analysis of PtPDIs

The multi-sequence alignment of PtPDIs was performed by mega 7.0 software (<http://www.megasoftware.net>). The multi-sequence alignment results were subsequently analyzed by the phylogenetic tree with 1000 bootstraps, and the phylogenetic tree was constructed to obtain the correlation among all PtPDIs. The evolutionary tree was finally optimized by Evolview (<https://www.evolgenius.info/evolview-v2/#login>). The motif structures of the PtPDI gene family were analyzed by multiple Em for motif elicitation website (MEME, <http://meme-suite.org>). The parameters were set to any number of repetitions. The optimal motif length was 6~10 amino acids. The time was 18,000 s. The maximum size was 6,000,000. The number of motifs was 10 and other parameters were the default values. The GFF file of *P. tricornutum* was used to screen the location information of CDS and UTR (untranslated region) of PtPDI genes on chromosomes. Finally, the software TBtools was used to visually integrate and improve the evolutionary tree, domain information, CDS, and UTR of PtPDI genes. The software map chart was used (<http://www.mapchart.net>) to draw the position of PtPDI genes on the chromosome.

2.2.3 Bioinformatic Prediction of PtPDIs

Signal peptide 3.0 (<https://services.healthtech.dtu.dk/service.php?SignalP-3.0>) and signal peptide 5.0 (<https://services.healthtech.dtu.dk/service.php?SignalP-5.0>) were applied to predict the signal peptide of PtPDIs. The transmembrane domain was predicted by TMHMM (<https://services.healthtech.dtu.dk/service.php?TMHMM-2.0>). The N-glycosylation site of PtPDI proteins was predicted by netnglyc-1.0 (<https://services.healthtech.dtu.dk/service.php?NetNGlyc-1.0>) and the subcellular localization of PtPDI proteins was determined by cell PLOC 2.0 website (<http://www.csbio.sjtu.edu.cn/bioinf/Cell-PLoc-2/>) and WoLF PSORT (<https://wolffpsort.hgc.jp/>), and further validated by Diatom specific HECTAR v1.3 (https://webtools.sb-roscoff.fr/root?tool_id=abims_hectar).

2.2.4 Tunicamycin Treatment and the Analysis of PtPDIs Expression in *P. tricornutum*

The 0.3 $\mu\text{mol L}^{-1}$ tunicamycin was used to treat the logarithmic growth stage of *P. tricornutum*. Transcriptomic analysis was carried out after 24 h of culture. The expression level of genes under the tunicamycin stress was analyzed and compared with that in the wild type. Genes' expression was processed by the Z-score method. The transcriptomic data was visualized by Heatmapper (<http://www.heatmapper.ca/>). Sequence reads are available on the NCBI sequence read archives [GSE209809]. The

data was published in our recent paper. Genes with $|\text{fold change}| \geq 1.5$ and $\text{FDR} < 0.01$ (adjusted p -value, determined by the Benjamini and Hochberg multiple-testing correction implemented in the ‘p. adjust’ method of R) were defined as differentially expressed genes. The value of FPKM was the average of the three biological replicates. Sequence reads are available on the NCBI sequence read archives [GSE209809]. The more detailed methods were reported in our recent paper [12].

3 Results

3.1 Identification and Classification of PtPDIs in *P. tricornutum*

Through the HMM search, 45 putative PtPDIs corresponding to the Pfam-thioredoxin family were obtained from the whole genome of *P. tricornutum*. After the manual confirmation by smart, NCBI CDD, and Pfam, 42 genes containing the thioredoxin domain were identified as PtPDIs. The 42 PtPDIs were named PtPDI1~PtPDI42, respectively (Table 1). The gene ID, signal peptide, transmembrane domain, N-glycosylation, and subcellular localization of these PtPDIs are shown in Table 1. Among them, 21 PtPDI proteins were predicted to contain signal peptides, while the other 21 PtPDI proteins did not have signal peptides. According to TMD prediction, the 12 of 42 PtPDI proteins had transmembrane domains. It was predicted that 23 of 42 PtPDI proteins contained N-glycosylation sites. PtPDI proteins were mainly predicted to target to endoplasmic reticulum, cytoplasm, chloroplast, and extracellular matrix. Some of them might be located in more than one subcellular organelle. For example, PtPDI25-27 might be located in the endoplasmic reticulum, mitochondrion, and cytoplasm.

Table 1: Bioinformatic characteristics of PtPDI genes

Name	Gene ID	SP	TMD	N-glycol	Subcellular localization
PtPDI1	Phatr3_J27972	No	No	No	Cytoplasm
PtPDI2	Phatr3_J46359	Yes	Yes	No	Endoplasmic reticulum
PtPDI3	Phatr3_J13505	No	No	Yes	Cytoplasm/Extra cell
PtPDI4	Phatr3_J13721	No	No	No	Cytoplasm/Nucleus
PtPDI5	Phatr3_J14096	No	No	Yes	Chloroplast/Cytoplasm
PtPDI6	Phatr3_J47306	Yes	No	No	Endoplasmic reticulum
PtPDI7	Phatr3_EG02276	Yes	No	Yes	Cytoplasm
PtPDI8	Phatr3_J21744	No	No	Yes	Cytoplasm
PtPDI9	Phatr3_J14885	No	Yes	Yes	Cytoplasm
PtPDI10	Phatr3_J14990	No	Yes	Yes	Endoplasmic reticulum
PtPDI11	Phatr3_J7656	No	No	Yes	Cytoplasm/Nucleus
PtPDI12	Phatr3_J15089	Yes	No	Yes	Cytoplasm
PtPDI13	Phatr3_J48643	No	No	Yes	Cytoplasm
PtPDI14	Phatr3_EG01957	Yes	No	Yes	Cytoplasm/Mitochondrion
PtPDI15	Phatr3_J43223	No	Yes	Yes	Nucleus/Golgi apparatus/Mitochondrion
PtPDI16	Phatr3_J9164	No	No	No	Mitochondrion/Cytoplasm
PtPDI17	Phatr3_J42566	Yes	No	No	Endoplasmic reticulum
PtPDI18	Phatr3_J43224	Yes	No	Yes	Vacuole

(Continued)

Table 1 (continued)

Name	Gene ID	SP	TMD	N-glycol	Subcellular localization
PtPDI19	Phatr3_EG01852	Yes	No	No	Endoplasmic reticulum
PtPDI20	Phatr3_J43106	No	Yes	No	Endoplasmic reticulum
PtPDI21	Phatr3_J8167	No	No	No	Cytoplasm
PtPDI22	Phatr3_J9171	Yes	Yes	No	Endoplasmic reticulum
PtPDI23	Phatr3_J48961	No	No	Yes	Chloroplast
PtPDI24	Phatr3_J49153	Yes	Yes	Yes	Chloroplast
PtPDI25	Phatr3_J49158	Yes	Yes	Yes	Endoplasmic reticulum/Mitochondrion
PtPDI26	Phatr3_J30502	No	No	Yes	Cytoplasm/Mitochondrion
PtPDI27	Phatr3_J7784	Yes	No	Yes	Chloroplast/Endoplasmic reticulum
PtPDI28	Phatr3_J50197	No	No	No	Cytoplasm
PtPDI29	Phatr3_J7528	Yes	No	Yes	Mitochondrion
PtPDI30	Phatr3_J33356	Yes	No	No	Cytoplasm/Endoplasmic reticulum
PtPDI31	Phatr3_EG02399	Yes	No	No	Cytoplasm/Vacuole
PtPDI32	Phatr3_J44590	No	Yes	Yes	Cytoplasm/Chloroplast
PtPDI33	Phatr3_J10788	Yes	No	Yes	Chloroplast/Mitochondrion
PtPDI34	Phatr3_J44374	No	No	No	Cytoplasm
PtPDI35	Phatr3_J2808	Yes	No	Yes	Endoplasmic reticulum
PtPDI36	Phatr3_J45252	Yes	Yes	No	Cytoplasm/Mitochondrion
PtPDI37	Phatr3_J11781	Yes	Yes	No	Endoplasmic reticulum
PtPDI38	Phatr3_J12104	Yes	No	Yes	Cytoplasm/Chloroplast
PtPDI39	Phatr3_J45921	No	No	Yes	Cytoplasm
PtPDI40	Phatr3_J8091	Yes	Yes	No	Cytoplasm/Chloroplast
PtPDI41	Phatr3_J9897	No	No	No	Cytoplasm
PtPDI42	Phatr3_J34741	No	No	No	Cytoplasm/Chloroplast

Note: ID: Gene identity; SP: signal peptide; TMD: trans-membrane domain; N-glyco: N-glycosylation.

3.2 Phylogenetic Analysis of PtPDI Genes

To investigate the evolutionary relationship among PtPDIs, the protein sequence of PtPDIs was used to map the phylogenetic tree through MEGA 7.0. Each PtPDI protein contained one or more thioredoxin domains. It was found that 42 PtPDI genes were divided into three branches according to the proteins' homology. In the pink branch, most PtPDI proteins had a thioredoxin domain. The homology of PtPDI17 and PtPDI19 was highest (94%). The homology of PtPDI34 and PtPDI42 and PtPDI36 was 95%. In the green branch, most PtPDI proteins had more than one thioredoxin domain. PtPDI39, PtPDI11, PtPDI13, and PtPDI29 had the highest homology, at about 80%. In the yellow branch, there were 3 PtPDI proteins with one thioredoxin domain and 3 PtPDI proteins with multiple thioredoxin domains (Fig. 1).

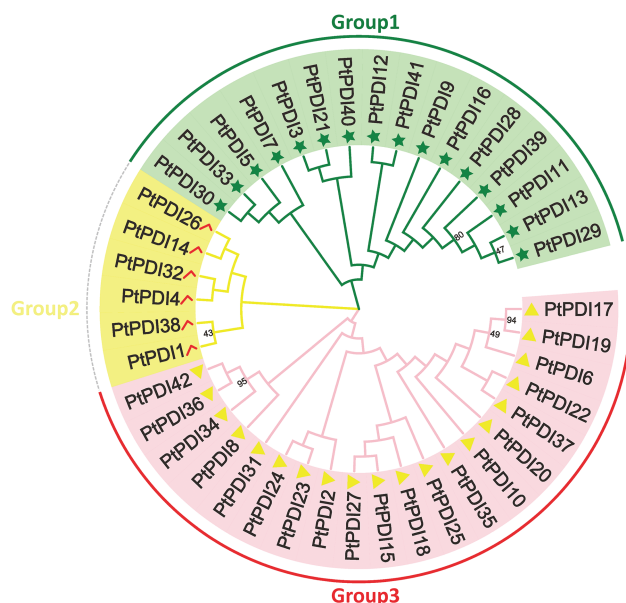


Figure 1: The phylogenetic tree of PtPDIs. Multi-sequence alignment was performed by Clustal W. Phylogenetic tree was constructed by Mega 7.0 software. And the multi-sequence alignment was analyzed by 1000 bootstrap

3.3 Characteristics of Conserved Domains in *P. tricornutum*

The analysis of gene structure and location, function, and evolution were shown. The whole genome of *P. tricornutum* was compared with the cDNA of PtPDI proteins to select the domain information and the coding sequences (CDS) (Fig. 2). It was observed that most PtPDI genes of *P. tricornutum* had multiple domains (Fig. 2). Except PtPDI1 without motif1, PtPDI28 and PtPDI32 without motif 2, all the other PtPDI genes contained motifs 1 and 2. Additionally, some PtPDI genes harbored some specific motifs, such as PtPDI20 and PtPDI35 with motifs 5, 6, and 9. 42 PtPDI genes had CDS structure (Fig. 2). Most of the genes had more than one exon. PtPDI35, PtPDI18, PtPDI16 and PtPDI13 genes contained three exons. The PtPDI20 gene harbored four exons. Based on the conserved domain, the 42 PtPDIs were classified into PDI-F (69%, 29/42), PDI-D (9.5%, 4/42), PDI-M (4.7%, 2/42), PDI-L (4.7%, 2/42), PDI-A (4.7%, 2/42), PDI-B (2.3%, 1/42) and PDI-C (2.3%, 1/42).

3.4 The Analysis of PtPDI Genes on the Chromosome

It was shown that the 42 PtPDI genes were distributed on 22 of 33 chromosomes of *P. tricornutum* (Fig. 3). There were 8 PtPDI genes located on chromosome 1. Moreover, the localization distance of PtPDI 15 and 18 genes was close on the chromosome. On chromosomes 4, 6, and 18, there were three PtPDI genes. In chromosome 1, there was a pair of tandem duplicate genes (PtPDI15 and PtPDI18 genes). On chromosome 6, there was a pair of PtPDI genes, named PtPDI42 and PtPDI37. There were 2 PtPDI genes on chromosomes 2, 3, 10, 13, 14, 17, 18 and 21. The location of the two PtPDI genes on chromosomes 14, 17, and 21 was adjacent. There was only one PtPDI gene on the other chromosomes.

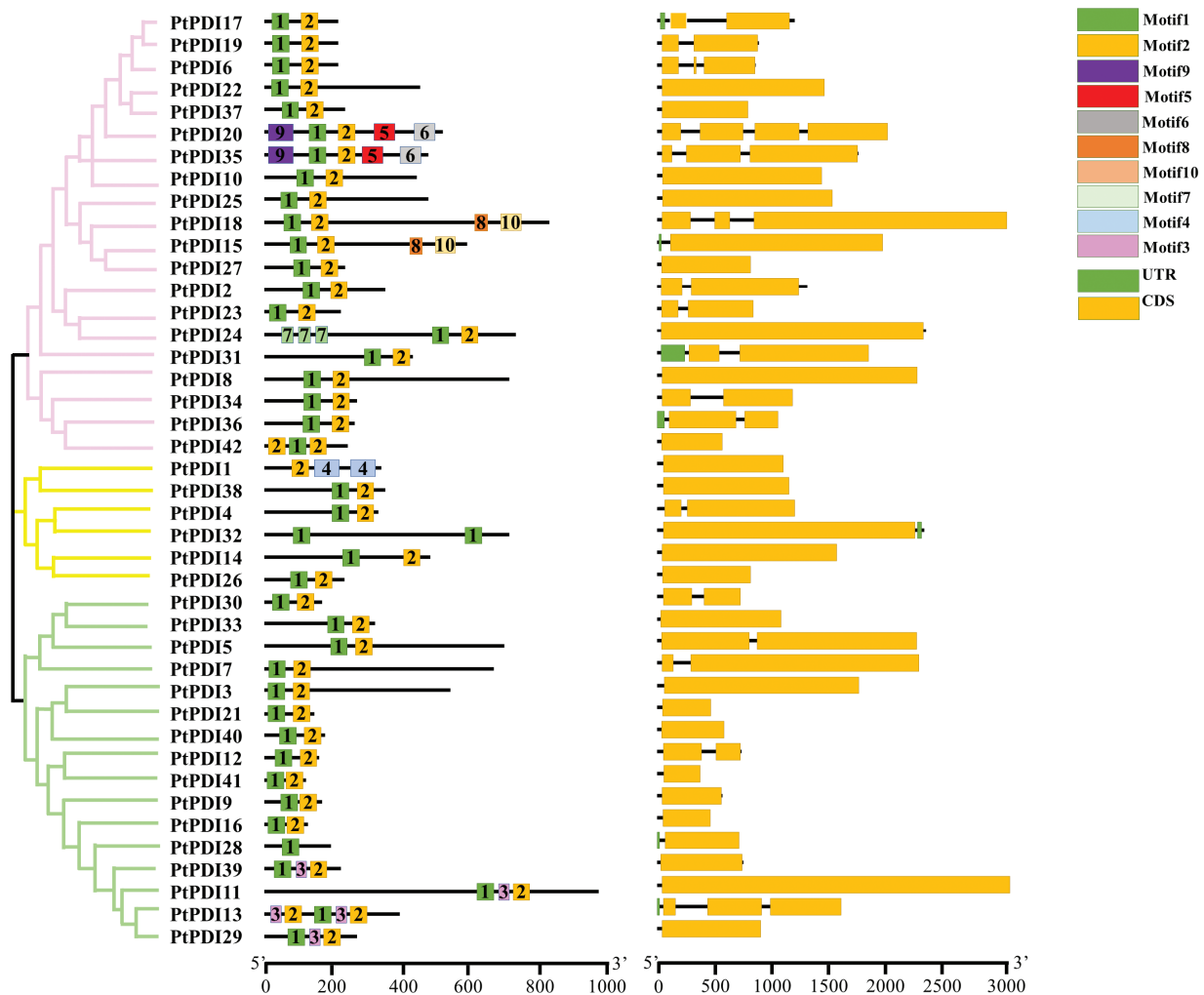


Figure 2: Phylogenetic tree, motif, and CDS sequence analysis of 42 PtPDIs. A Phylogenetic tree was optimized via mega 7.0 software with 1000 bootstrap. B, the motif structure of PtPDIs was shown by the MEME website. Each motif was represented by a color. The number in the box is the serial number of the motif type. The length of PtPDI genes was observed through the scale line at the bottom. C, CDS was represented in the yellow box, and UTR was represented in the green box

3.5 Expression Characteristics of PtPDI Genes under Tunicamycin Stress

To further analyze the expression of PtPDI genes, the transcription level of PtPDI genes was studied under the $0.3 \mu\text{mol L}^{-1}$ tunicamycin treatment. The expressional heatmap is shown in Fig. 4. Compared to the expression of PtPDIs in the wild type, 14 PtPDI genes were up-regulated. They were PtPDI1, PtPDI4-5, PtPDI7, PtPDI11-12, PtPDI15, PtPDI17, PtPDI22, PtPDI29, PtPDI35-37 and PtPDI42 genes. The fold change of upregulated PtPDI11 and PtPDI42 genes was more than 1.5. Conversely, 7 genes were significantly down-regulated after the treatment of $0.3 \mu\text{mol L}^{-1}$ tunicamycin. They were PtPDI6, PtPDI13, PtPDI16, PtPDI31, PtPDI33, PtPDI40 and PtPDI41 genes.

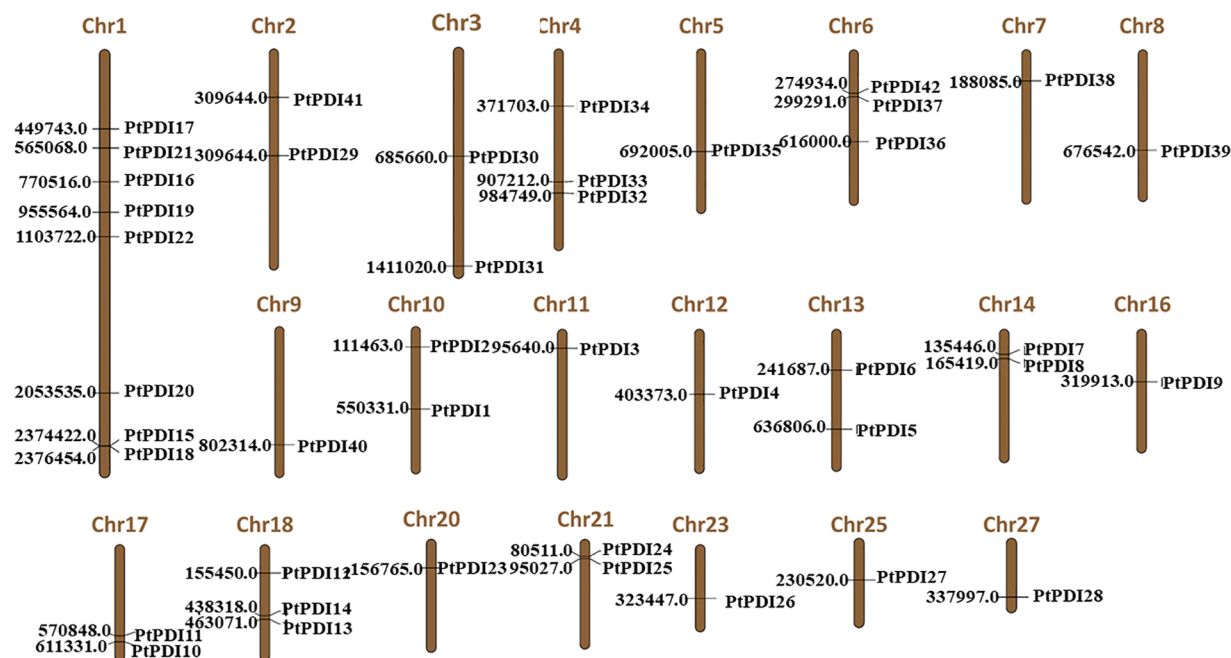


Figure 3: Localization of PtPDI genes on chromosomes. The number of each chromosome was shown on the top of the chromosome. The number on the left was the position of PtPDI genes on the chromosome

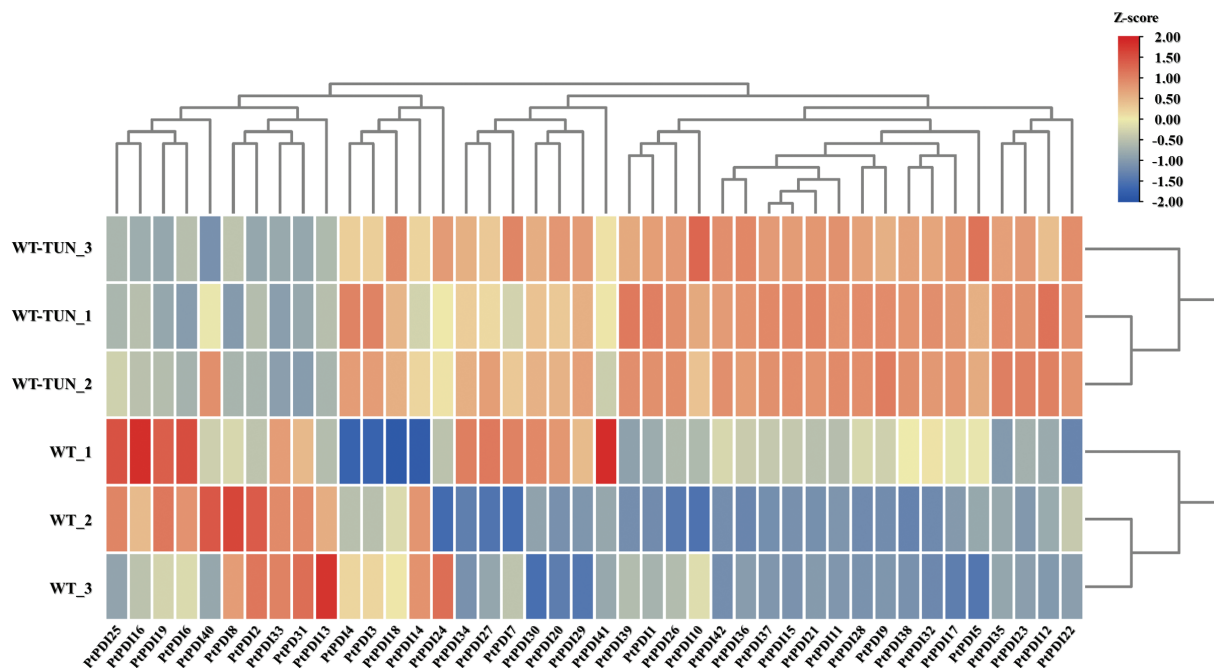


Figure 4: Transcription level of PtPDI genes under the treatment of 0.3 $\mu\text{mol L}^{-1}$ tunicamycin in *P. tricornutum*. WT represents wild-type, and WT-TUN represents 0.3 $\mu\text{mol L}^{-1}$ tunicamycin treatment. The expression of genes was processed by the Z-score method. Genes with $|\text{fold change}| \geq 1.5$ and $\text{FDR} < 0.01$ (adjusted p -value, determined by the Benjamini and Hochberg multiple-testing correction implemented in the 'p. adjust' method of R) were defined as differentially expressed genes

4 Discussion

In this study, 42 PtPDI candidates were identified from *P. tricornutum*. However, only 8 CrPDIs were identified from the genome of *C. reinhardtii*, and 10 OsPDIs were observed in *Ostreococcus lucimarinus* [21]. The different number of PDIs might be dependent on the algal species. Many more PtPDI in *P. tricornutum* were identified here, indicating that Diatom might need more PDIs to regulate the complex ERQC pathway. In high plants, PDI proteins were classified into nine classes, including PDI-A, PDI-S, PDI-E, PDI-B, PDI-C, PDI-M, PDI-D, and PDI-F. The difference between these 9 PDI classes was the number and the position of the Trx domain and the presence of additional domains [14]. Previous reports showed that PDI-A in *Arabidopsis thaliana* could bind an iron-sulfur (Fe-S) cluster. It was certified that this binding scavenged the free iron to prevent the production of reactive oxygen [22]. PDI-M from plant *Populus trichocarpa x Populus deltoides* had the ability of oxidation-reduction regulation to activate the NADP-MDH [23]. This indicated that different kinds of PDIs played diverse roles. It was reported that PDI-F was found in microalgae, such as *C. reinhardtii*, *Thalassiosira pseudonana*, and *Emiliania huxleyi* [14,21,24]. Previous papers showed that three PDI-F proteins were found in diatom *T. pseudonana* [14,21]. Differently, 27 PtPDI-F subfamily was found in *P. tricornutum* in this study. These results enriched the PDI-F subfamily, and it was indicated that the number of PDIs was species-specific. At the same time, it was found that PDIs were divided into different groups. For example, in *Brassica rapa ssp. Pekinensis*, 32 PDIs were clustered into PDI-A (15.6%, 5/32), PDI-L (34.3%, 11/32), PDI-C (18.7%, 6/32), PDI-S (6.25%, 2/32), PDI-M (6.25%, 2/32), PDI-D (6.25%, 2/32), and PDI-E (12.5%, 4/32) [25]. In *Arabidopsis thaliana*, 21 PDIs were grouped into PDI-A (19%, 4/21), PDI-L (33.3%, 7/21), PDI-C (14.28%, 3/21), PDI-S (4.7%, 1/21), PDI-M (9.5%, 2/21), PDI-D (9.5%, 2/21) and PDI-E (9.5%, 2/21) [25]. 17 PDIs from *Medicago truncatula* belonged to PDI-L (29.4%, 5/17), PDI-S (23.5%, 4/17), PDI-C (17.6%, 3/17), PDI-B (5.8%, 1/17), PDI-A (5.8%, 1/17), PDI-E (5.8%, 3/17) [25,26]. 8 PDIs identified from *C. reinhardtii* were clustered into PDI-E (12.5%, 1/8), PDI-C (12.5%, 1/8), PDI-L (12.5%, 1/8), PDI-S (12.5%, 1/8), PDI-M (12.5%, 1/8), PDI-D (12.5%, 1/8) and PDI-F (25%, 2/8) [21]. In a previous paper, 7 PtPDIs were identified by blast search in the genome, including 1 PtPDI-B, 2 PtPDI-C, 1 PtPDI-E, and 4 PtPDI-F [14]. Many more PtPDIs (4 PtPDI-B, 4 PtPDI-C, 2 PtPDI-E, 27 PtPDI-F, 5 PtPDI-L) were identified via the Pfam number in this study, indicating a further method was important for the genome wild research. It was also proposed that more PtPDIs in *P. tricornutum* were needed to adapt to complex environments during secondary endosymbiosis.

Except PtPDI1, all the other PtPDIs contained motif 1 and motif 2 in *P. tricornutum* in this study, indicating that these two motifs were critical for the function of PtPDIs. Similarly, motif 1 and motif 2 were also highly conserved in rice [27]. Additionally, it was reported that motif 1 and motif 2 were responsible for the resistance of plant *Panax ginseng* to environmental stresses, such as drought [27,28]. Therefore, it was speculated that these two motifs in *P. tricornutum* might have a similar function under environmental pressures. In this study, 42 PtPDIs were located in different subcellular organelles, including cytoplasm, endoplasmic reticulum, Golgi apparatus, chloroplast, and nucleus. Consistent with the previous reports [14,29], ER-localized PtPDIs also contained ER retention signal, for example, PtPDI17 contained KEEL at the C-terminus, and PtPDI19 had EDEL motif. The subcellular localization of PtPDIs in *C. reinhardtii* was similar to that in *P. tricornutum* [30]. This suggested that PtPDIs were widely distributed into different subcellular organelles and played different functions in these diverse structures. However, all these putative localizations needed experiments to certify, such as via the observation of PtPDIs-eGFP fluorescence in confocal laser scanning microscopy. It was also found that PtPDIs played a vital role in forming disulfide bonds and modifying misfolded proteins in ER [31]. Moreover, it has been shown that PDIs could regulate thiol-disulfide switches and help repair the cytoskeleton in cell surface and cytosol [32]. Hence, ER-localized PtPDIs might also participate in the formation of disulfide bonds in proteins and regulate the correct folding of misfolded/unfolded proteins to

maintain protein homeostasis in the cell. However, the exact function of these PtPDIs needs more experiments to clarify, such as by the overexpression, knock-out, and/or knockdown of genes in *P. tricornutum*.

A previous study reported that gene-duplicated events played an important role in the rapid expansion and evolution of gene families [33]. Gene-duplicated events usually happen among most plants and algae [34]. A pair of tandem duplicated genes (PtPDI15 and PtPDI18 genes) was observed in the genome of *P. tricornutum*. At the same time, it was observed that the gene structure, motifs, and homology of these two genes were highly conserved, indicating that these two PtPDIs might have similar functions in *P. tricornutum*. Compared to the reported homologous gene PDI-L5-1 (At1g04980) with two CXXC motifs in *Arabidopsis thaliana* [14,35], both PtPDI15 and PtPDI18 contained three CXXC motifs, indicating the structure specificity among different organisms. WP1 in yeast *Rhodotorula gramini*, a homologous gene of PtPDI15 and PtPDI18, could increase resistance and tolerance against a wide range of biotic and abiotic stresses, such as oxidative stress and heavy metals [34]. The homologous genes of PtPDI15 and PtPDI18 in the fungus *Wallemia* played an important role in osmoregulation under the hyperosmotic environment [36]. These studies suggested that PtPDI15 and PtPDI18 genes might also be important for the responses of *P. tricornutum* under the biotic and abiotic stresses, such as tunicamycin stress in this study.

It was known that PDIs play a crucial role in aiding the correct folding and assembly of nascent proteins in ERQC to maintain protein and cellular homeostasis. ERQC is an important pathway in ER (Fig. 5) [7]. Two ER-located PDI proteins were reported to be related to ER stress in Soybeans [15,37]. In this paper, PtPDI6, 17, 19, 20, 22, 35, and 37 with ER retention motif were predicted to be located in ER, therefore, it was reasonable to propose that these 7 PtPDIs might be involved in the ERQC pathway to resist ER stress and maintain cellular protein and cellular homeostasis. Moreover, it was found that the expression of these PtPDI genes was different under the stress of tunicamycin. Tunicamycin is an effective protein inhibitor, affecting the N-glycosylation modification of proteins and causing the accumulation of unfolded and/or misfolded proteins in the ER lumen [20,38]. PtPDI genes were differentially expressed to respond to the tunicamycin stress. Similar results were observed in tomato and *Chlamydomonas* [39]. The differential expression of PDI genes was dependent on the activation or repression of transcription factors. It was reported that bZIPs played a key role in the regulation of expression of PDI genes [29], therefore, it was speculated that the differentially expressed PtPDIs were regulated by different bZIP transcription factors. In this paper, it was suggested that the up-regulated PtPDIs (PtPDI11, PtPDI4-5, PtPDI7, PtPDI11-12, PtPDI15, PtPDI17, PtPDI22, PtPDI29, PtPDI35-37, and PtPDI42) might be involved in maintaining cellular protein homeostasis as positive regulatory factors. This suggestion was verified by that the homologous genes of PtPDI15 played important roles in cellular homeostasis, especially under oxidative, heavy metal, and hyperosmotic stresses [40]. The homologous gene Rb60/PDI1A of PtPDI22 in *C. reinhardtii* was also strongly upregulated in response to tunicamycin treatment, and it was also found that both Rb60/PDI1A and PtPDI22 were putatively targeted to ER [39,41]. The second homologous gene PDI6 in *C. reinhardtii* of PtPDI1 was also dramatically upregulated in tunicamycin-treated cells, indicating that this gene was involved in the cellular response to this stress [39]. The homologous relationship is shown in Supplementary Fig. 1. However, the downregulated PtPDIs (PtPDI6, PtPDI13, PtPDI16, PtPDI31, PtPDI33, PtPDI40 and PtPDI41) might act as negative regulatory factors. However, the negative regulatory mechanism of PtPDIs in *P. tricornutum* was still unknown. The homologous genes AtPDI2/5 of PtPDI6/16 showed the same differentially expressed profiles, indicating that these two PtPDIs might have synergistically functioned as AtPDI2/5 on the formation of a disulfide bond [42]. The differentially expressed PtPDIs could also be explained by that tunicamycin induced the unfolded protein response (UPR), and then UPR affected the transcription of PtPDIs [29]. In our recent paper, it was concluded that the differentially expressed PDI genes in *C. reinhardtii* might also play an important role in the response to Pb stress [21]. Anyway, it was proposed

that these PtPDI genes might act as a catalyst of disulfide bond formation, helping stabilize protein folding's tertiary and quaternary structures and maintaining cellular homeostasis during various stresses.

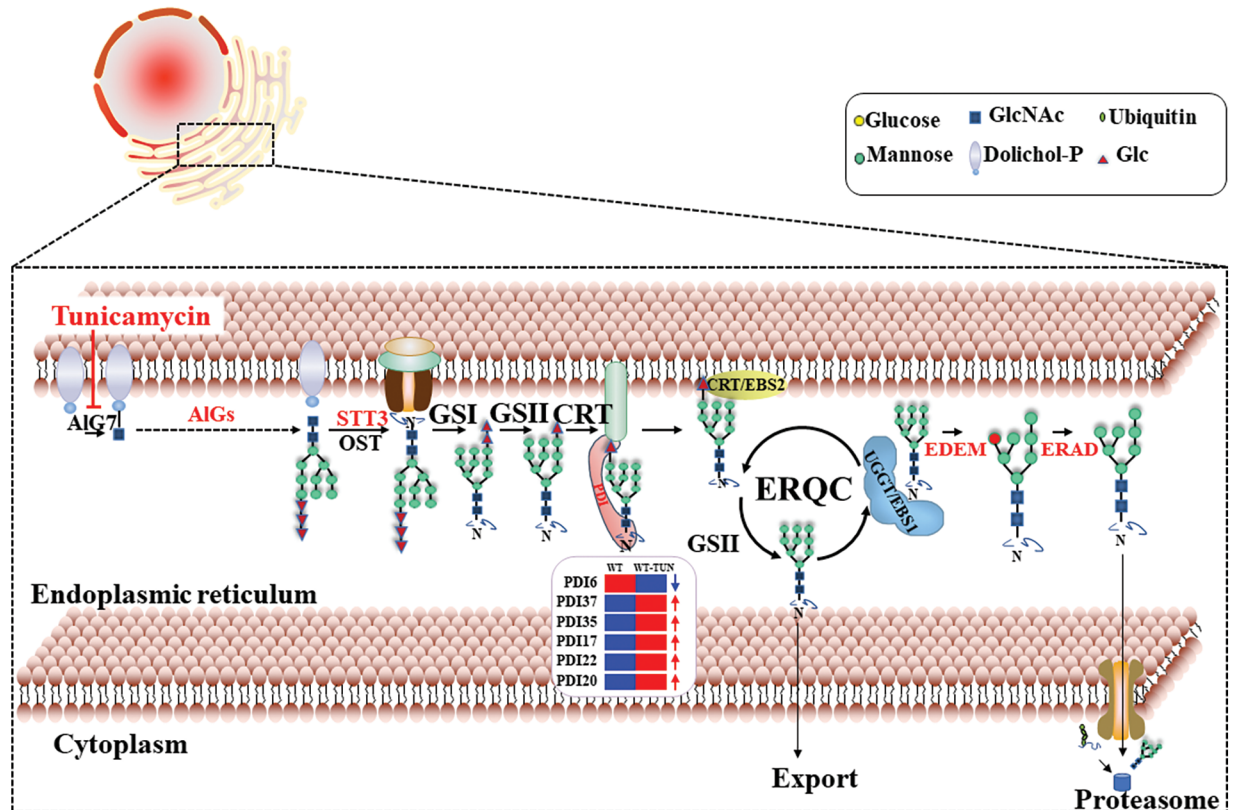


Figure 5: The working model of PtPDIs during the ERQC pathway in *P. tricornutum*. PtPDI6, 17, 19, 20, 22, 35, and 37 genes were predicted to be located in ER. The blue arrow means the downregulation and the red arrows mean the upregulation of PtPDI genes under the tunicamycin treatment

Acknowledgement: Thanks to the funding of Educational and Scientific Research Projects for Young and Middle-Aged Teachers in Fujian Province, Natural Science Foundation of Guangdong Province, the Program for University Innovation Team of Guangdong Province, National Natural Science Foundation of China, and the Innovation and Entrepreneurship Project of Shantou.

Funding Statement: Thanks to the funding of Educational and Scientific Research Projects for Young and Middle-Aged Teachers in Fujian Province (Grant Number: 2022JAT220693), Natural Science Foundation of Guangdong Province (Grant Number: 2022A1515012141), the Program for University Innovation Team of Guangdong Province (Grant Number: 2022KCXTD008), National Natural Science Foundation of China (92158201 and 42376001) and the Innovation and Entrepreneurship Project of Shantou (201112176541391).

Author Contributions: X. Liu designed the experiments and supervised the project. Y. Lin, H. Du, and Z. Ye performed the experiments and analysed the data. Y. Lin, H. Du, S. Wang, Z. Wang and X. Liu wrote and revised the manuscript. All authors discussed the results and implications and commented on the manuscript at all stages.

Availability of Data and Materials: All data generated or analysed during this study are included in this published article.

Ethics Approval: Not applicable.

Conflicts of Interest: The authors declares that they have no conflicts of interest to report regarding the present study.

Supplementary Materials: The supplementary material is available online at <https://doi.org/10.32604/phyton.2023.044996>.

References

1. Edkins AL, Boshoff A. General structural and functional features of molecular chaperones. *Advan Experi Med Biol.* 2021;1340:11–73.
2. Lee S, Tsai FT. Molecular chaperones in protein quality control. *J Biochem Molecul Biol.* 2005;38:259–65.
3. Winter J, Jakob U. Beyond transcription—new mechanisms for the regulation of molecular chaperones. *Critical Reviews Biochem Molecul Biol.* 2004;39:297–317.
4. Hartl FU, Bracher A, Hayer-Hartl M. Molecular chaperones in protein folding and proteostasis. *Nature.* 2011;475:324–32.
5. Lia A, Gallo A, Marti L, Roversi P, Santino A. EFR-mediated innate immune response in *Arabidopsis thaliana* is a useful tool for identification of novel ERQC modulators. *Genes.* 2018;10:9–10.
6. Marti L, Lia A, Reza IB, Roversi P, Santino A et al. Planta preliminary screening of ER glycoprotein folding quality control (ERQC) modulators. *IJMS.* 2018;19:9–7.
7. Tax G, Lia A, Santino A, Roversi P. Modulation of ERQC and ERAD: A broad-spectrum spanner in the works of cancer cells? *J Oncol.* 2019;2019:8384913.
8. Hashimoto S, Okada K, Imaoka S. Interaction between bisphenol derivatives and protein disulphide isomerase (PDI) and inhibition of PDI functions: Requirement of chemical structure for binding to PDI. *J Biochem.* 2008;144:335–42.
9. Oliveira PVS, Garcia-Rosa S, Sachetto ATA, Moretti AIS, Debbas V et al. Protein disulfide isomerase plasma levels in healthy humans reveal proteomic signatures involved in contrasting endothelial phenotypes. *Redox Biol.* 2019;22:101142.
10. Ellgaard L, Ruddock LW. The human protein disulphide isomerase family: Substrate interactions and functional properties. *Embo Reports.* 2005;6:28–32.
11. Laurindo FR, Pescatore LA, Fernandes Dde C. Protein disulfide isomerase in redox cell signaling and homeostasis. *Free Radi Biol Med.* 2012;52:1954–69.
12. Chen J, Du H, Liu Z, Li T, Du H et al. Endoplasmic reticulum-quality control pathway and endoplasmic reticulum-associated degradation mechanism regulate the N-glycoproteins and N-glycan structures in the diatom *Phaeodactylum tricorutum*. *Microb Cell Fact.* 2022;21:219.
13. Firrincieli A, Otilar R, Salamov A, Schmutz J, Khan Z et al. Genome sequence of the plant growth promoting endophytic yeast *Rhodotorula graminis* WP1. *Fronti Microbiol.* 2015;6:978.
14. Selles B, Jacquot JP, Rouhier N. Comparative genomic study of protein disulfide isomerases from photosynthetic organisms. *Genom.* 2011;97:37–50.
15. Okuda A, Matsusaki M, Masuda T, Urade R. Identification and characterization of GmPDIL7, a soybean ER membrane-bound protein disulfide isomerase family protein. *Febs J.* 2017;284:414–28.
16. Wai AH, Waseem M, Khan A, Nath UK, Lee DJ et al. Genome-wide identification and expression profiling of the PDI gene family reveals their probable involvement in abiotic stress tolerance in tomato (*Solanum lycopersicum* L.). *Genes.* 2020;12:6–7.
17. Araie H, Shiraiwa Y. Selenium utilization strategy by microalgae. *Molecules.* 2009;14:4880–91.

18. Hempel F, Lau J, Klingl A, Maier UG. Algae as protein factories: Expression of a human antibody and the respective antigen in the diatom *Phaeodactylum tricornutum*. PLoS One. 2011;6:e28424.
19. Faheem M, Arshad M, Xiao JIN, Wang H, Li Y et al. Cloning and functional assessment of the protein disulfide isomerase (PDI-V) gene and its promoter sequences from *Haynaldia villosa*. Turkish J Bot. 2018;42:9–10.
20. Xiao H, Smeeckens JM, Wu R. Quantification of tunicamycin-induced protein expression and N-glycosylation changes in yeast. Analyst. 2016;141:3737–45.
21. Du H, Zheng C, Aslam M, Xie X, Wang W et al. Endoplasmic reticulum-mediated protein quality control and endoplasmic reticulum-associated degradation pathway explain the reduction of N-glycoprotein level under the lead stress. Front Plant Sci. 2020;11:598552.
22. Remelli W, Santabarbara S, Carbonera D, Bonomi F, Ceriotti A et al. Iron binding properties of recombinant class a protein disulfide isomerase from *Arabidopsis thaliana*. Biochem. 2017;56:2116–25.
23. Selles B, Zannini F, Couturier J, Jacquot JP, Rouhier N. Atypical protein disulfide isomerases (PDI): Comparison of the molecular and catalytic properties of poplar PDI-A and PDI-M with PDI-L1A. PLoS One. 2017;12:e0174753.
24. Obata T, Shiraiwa Y. A novel eukaryotic selenoprotein in the haptophyte alga *Emiliania huxleyi*. J Biol Chem. 2005;280:18462–8.
25. Kayum MA, Park JI, Nath UK, Saha G, Biswas MK et al. Genome-wide characterization and expression profiling of PDI family gene reveals function as abiotic and biotic stress tolerance in Chinese cabbage (*Brassica rapa* ssp. *pekinensis*). BMC Genom. 2017;18:885.
26. Meng Z, Zhao Y, Liu L, Du X. Genome-wide characterization of the PDI gene family in *Medicago truncatula* and their roles in response to endoplasmic reticulum stress. Genome. 2021;64:599–614.
27. Zhang Q, Shen L, Ren D, Hu J, Zhu L et al. Characterization of the CRM gene family and elucidating the function of OsCFM2 in rice. Biomole. 2020;10:6–7.
28. Bae KS, Rahimi S, Kim YJ, Devi BSR, Khorolragchaa A et al. Molecular characterization of lipoxygenase genes and their expression analysis against biotic and abiotic stresses in *Panax ginseng*. Eur J Plant Pathol. 2016;145:331–43.
29. Gupta D, Tuteja N. Chaperones and foldases in endoplasmic reticulum stress signaling in plants. Plant Signal Behav. 2011;6:232–6.
30. Reyes S, Moreno A. The endoplasmic reticulum role in the plant response to abiotic stress. Front Plant Sci. 2021;12:1–7.
31. Määttänen P, Gehring K, Bergeron JJ, Thomas DY. Protein quality control in the ER: The recognition of misfolded proteins. Seminars Cell Develop Biol. 2010;21:500–11.
32. Soares Moretti AI, Martins Laurindo FR. Protein disulfide isomerases: Redox connections in and out of the endoplasmic reticulum. Arch Biochem Biophys. 2017;617:106–19.
33. Freeling M. Bias in plant gene content following different sorts of duplication: Tandem, whole-genome, segmental, or by transposition. Ann Rev Plant Biol. 2009;60:433–53.
34. Qiao X, Li Q, Yin H, Qi K, Li L et al. Gene duplication and evolution in recurring polyploidization-diploidization cycles in plants. Genome Biol. 2019;20:38.
35. Zhou Y, Fan F, Han Y, Lu D. Arabidopsis PDI11 interacts with lectin molecular chaperons calreticulin 1 and 2 through its D domain. Biochem Biophys Research Comm. 2022;588:55–60.
36. Padamsee M, Kumar TK, Riley R, Binder M, Boyd A et al. The genome of the xerotolerant mold *Wallemia sebi* reveals adaptations to osmotic stress and suggests cryptic sexual reproduction. Fungal Genet Biol. 2012;49:217–26.
37. Okuda A, Matsusaki M, Masuda T, Morishima K, Sato N et al. A novel soybean protein disulphide isomerase family protein possesses dithiol oxidation activity: Identification and characterization of GmPDIL6. The J Biochem. 2020;168:393–405.

38. McCormick LM, Urade R, Arakaki Y, Schwartz AL, Bu G. Independent and cooperative roles of N-glycans and molecular chaperones in the folding and disulfide bond formation of the low-density lipoprotein (LDL) receptor-related protein. *Biochem.* 2005;44:5794–803.
39. Pérez-Martín M, Pérez-Pérez ME, Lemaire SD, Crespo JL. Oxidative stress contributes to autophagy induction in response to endoplasmic reticulum stress in *Chlamydomonas reinhardtii*. *Plant Physiol.* 2014;166:997–1008.
40. Zhao C, Shono M, Sun A, Yi S, Li M et al. Constitutive expression of an endoplasmic reticulum small heat shock protein alleviates endoplasmic reticulum stress in transgenic tomato. *J Plant Physiol.* 2007;164:835–41.
41. Levitan A, Trebitsh T, Kiss V, Pereg Y, Dangoor I et al. Dual targeting of the protein disulfide isomerase RB60 to the chloroplast and the endoplasmic reticulum. *PNAS.* 2005;102:6225–30.
42. Fan F, Zhang Q, Zhang Y, Huang G, Liang X et al. Two protein disulfide isomerase subgroups work synergistically in catalyzing oxidative protein folding. *Plant Physiol.* 2022;188:241–54.